IV International Conference on Computational Methods for Coupled Problems in Science and Engineering
COUPLED PROBLEMS 2011
M. Papadrakakis, E. Oñate and B. Schrefler (Eds)

ELECTROSTATIC DIAPHRAGM MICROPUMP ELECTRO-FLUID-MECHANICAL SIMULATION

EMANUELE BERTARELLI, RAFFAELE ARDITO AND ALBERTO CORIGLIANO

Department of Structural Engineering, Politecnico di Milano,
Piazza Leonardo da Vinci 32, 20133 Milano, Italy
e-mail: bertarelli@stru.polimi.it

Key words: Electrostatic micropump, Multiphysics simulation, Electro-fluid-mechanical coupling, Biological micro-electro-mechanical systems (BioMEMS)

Abstract. In this work, a fully-silicon mechanical displacement micropump is proposed and investigated. Electrostatic actuation of a flexible diaphragm is used to generate the pressure difference required to transport the fluid at the microscale. The study is carried out by exploiting the Finite Element method in a multiphysics framework, considering simplified geometries and boundary conditions. These investigations suggest the possibility to adopt the proposed device for applications in biomedical and biological fields. Achievable stroke volumes and flow rates are computed: values are in line with those obtained for similar devices presented in the literature.

1 INTRODUCTION

Micropumping is emerging as a critical research area for many applications. Several extensive reviews concerning micropumps are available [1–3]; some of them have emphasized specific applications [4–6]. The motivations of this growing interest in micropumping can be found first in the need to develop miniaturized pumping mechanisms for applications in microfluidics. Indeed, a major research interest in this area is the development of autonomous platforms to perform a precise manipulation of biological samples or the administration of drugs and chemicals. It is worth mentioning that microfluidics is also an essential part of precision control systems for automotive, aerospace and machine tool industries [4]. Additionally, micropumps are being considered for applications in the thermal management of electronic components [6].

Nevertheless, the industrial transfer is still at the beginning. Some micropumps have already entered the marketplace, but to definitely obtain a broad diffusion, cost-optimised and fabrication-optimised designs and a good performance reproducibility are the next goals to be achieved [2]. The key step at this point is to perform technology-driven

studies, in which a micropumping principle is developed in the framework of a well-established fabrication technology. In particular, the perspective of taking advantage of MEMS Integrated Circuits batch-processing technology to obtain affordable and reliable devices is of great interest. Besides, a direct integration with electronic components can be achieved, which is a key feature for power supplying and control of the device, as well as for a straightforward embedding in the electronic devices to be cooled or the realization of devices for fluid actuation and manipulation along the same fabrication process [7]. Indeed, the possibility to realize effective microfluidic components with MEMS microfabrication technology has been proven [8].

In this work, a diaphragm displacement micropump is proposed. The motion of a flexible diaphragm through electrostatic actuation is used to generate a pressure difference and then to obtain the fluid transport. The electrostatic actuation is considered, since this choice shows some relevant advantages, such as low power consumption, fast response time and full MEMS compatibility [2]. Since no external actuation is required, the cost and complexity of the device is noticeably reduced with respect to other actuation solutions (e.g. piezoelectric). The main reference for device actuation design is the work by Zengerle *et al.* [9]. However, a different geometry is here proposed and the stable operation regime – avoiding actuator electrostatic collapse – is considered.

The micropump here presented is intended to be used for biomedical applications – such as drug delivery systems – or for microfluidics devices for biological fluid handling and analysis. Key requirements are high quality standards and low costs, since many drug delivery systems and biological analytical chips are disposable. In these contexts, the possibility to exploit microsystems fabrication to obtain cost-effective manufacturing in high volume, satisfying high requirements of accuracy and reliability, is a fundamental aspect and represents a research driving force. Biocompatibility issues have to be considered too, especially for implantable devices or components that are directly interfaced with the biological environment [10].

2 DEVICE DESIGN

The geometry of the in-silicon micropumping device under study is reported in Figure 1. A description of a micromachining process suitable to realize it is reported elsewere [7]. A circular pumping chamber with $R = 2$ mm radius and $h_f = 10$ μm height is designed. The initial volume of the pumping chamber is $v_0 = \pi R^2 h_f \simeq 126$ nl. The diaphragm is realized in polysilicon, with a thickness h_m. A rigid ground electrode is placed above, with spacing h_c. The space between electrodes is assumed to be filled of a dielectric, namely air, with permittivity ε. The actuation voltage is such that $V_{max} = 60$ V.

Inlet and outlet ports are placed along the perimeter of the pumping chamber, in diametrically opposite positions. At this stage ideal valves are considered, with no pressure drop during fluid flow and no leakage if valve is closed. Herein, inlet pressure is referred as p_{in} and outlet pressure is referred as p_{out}. Inlet pressure can be regarded as the pressure of a reservoir which contains the fluid to be pumped, even pressurized to facilitate pumping.

The device functioning over a pumping cycle is illustrated in Figure 2. Starting from the rest position (a), when voltage is applied the diaphragm is loaded by an electrostatic pressure. This pressure is transferred to the fluid contained in the pumping chamber and generates a depression. When the chamber pressure is lower than the inlet pressure, the inlet valve opens and liquid flows into the expanding chamber (expansion stroke), while the diaphragm deflects as a consequence of the electrostatic force acting on it (b). When voltage is removed, the diaphragm bounces back. This increases the pressure in the pumping chamber (compression stroke). When the chamber pressure is higher than the outlet pressure, an amount of liquid is discharged through the outlet valve (c). In fact, the driving force in the emptying phase is given by the elastic recovery of the diaphragm.

For a generic pumping cycle, after fluid discharge the pressure in the pumping chamber will be equal to p_{out}. Indeed, the outlet valve closes when the pressure inside the pumping chamber is equal to the outlet pressure, since the system has reached an equilibrium condition. The pressure difference to overcome during the next filling is then $p_{out} - p_{in}$. Conversely, the pressure in the pumping chamber at the end of filling is p_{in}, then the pressure difference to overcome is then again $p_{out} - p_{in}$. Summarizing, since ideal valves are considered, the pressure drop to overcome during a pumping cycle, in both expansion and compression stroke, is given by the difference between the outlet pressure p_{out} and the inlet pressure p_{in}:

$$\Delta p = p_{out} - p_{in} \tag{1}$$

On the assumption that all the charges are localized within a thin layer below the electrode surface and that there is no bending of the diaphragm towards the counterelectrode, a lower limit for the electrostatic generated pressure is [9]

$$\tilde{p}_{el} = \frac{\varepsilon V^2}{2\, h_c^2} \tag{2}$$

Equation 2 represents the minimum value of the electrostatic force, calculated in rest position. Once the diaphragm deflects, the distance between the plates decreases and an higher (although non-uniform) pressure is exerted on the diaphragm on the new configuration [11].

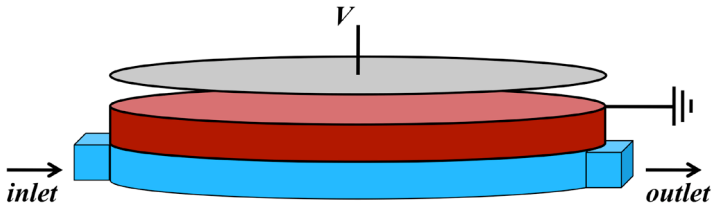

Figure 1: The proposed device design. Rigid electrode (upper gray plate), diaphragm (in red) and pumping chamber (in blue) are represented (not to scale).

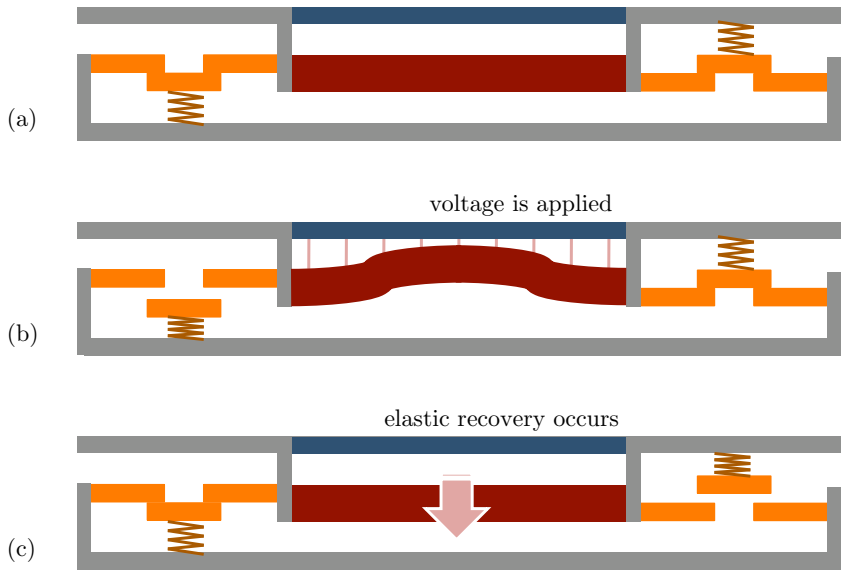

Figure 2: Device functioning over a pumping cycle: rest position (a), filling (b) and fluid discharge (c). Valve action is schematically represented.

To start a pumping cycle, the actuator electrostatic pressure in rest position must be higher than Δp. This is required to generate a sufficient chamber depression to open the inlet valve. This condition can be represented by the inequality

$$\frac{\varepsilon V^2}{2 h_c^2} > \Delta p \tag{3}$$

Equation 3 expresses a minimum requirement. If matched, the diaphragm starts to move and the electrostatic pressure to rise, up to the desired deflection (Figure 3). In this study, inlet and outlet pressure is the same: $\Delta p = 0$ [9].

Fluid discharge is obtained in the proposed device by elastic recovery only. In previous works on micropumps simulation [12; 13], when outlet and inlet pressure is considered to be the same, the pumping chamber variation in quasi-static conditons v_s was assumed as stroke volume Δv, considering that the diaphragm ideally bounces back to the undeformed configuration at each pumping cycle:

$$\Delta v \simeq v_s \tag{4}$$

Then, for a given pumping frequency f_p, the ideal flow should be given by

$$\mathcal{Q}_i = v_s \cdot f_p \tag{5}$$

If this approach is applied to the device here investigated, a theoretical flow transport capability of $\mathcal{Q}_i$ = 1-15 μl/min for an actuation frequency of 10-50 Hz is estimated [7; 11].

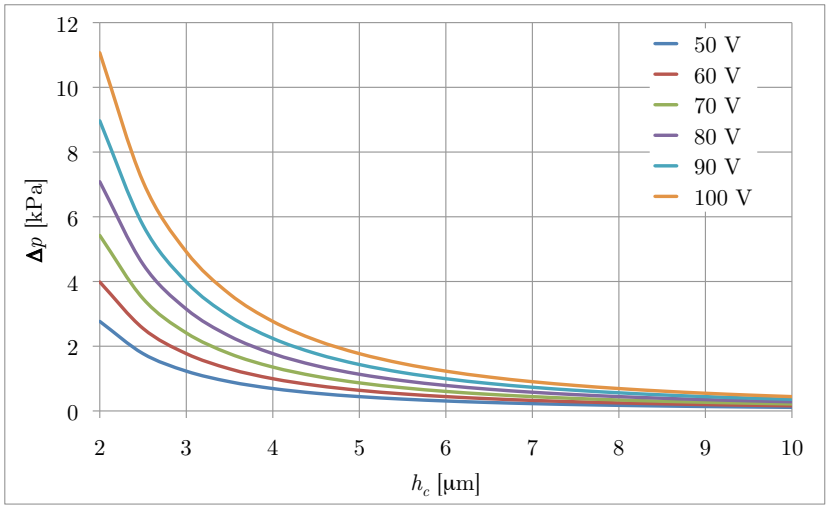

Figure 3: Limit value of the pressure drop $\Delta p = p_{out} - p_{in}$ that can be overcome, for different applied voltages and capacitor spacings.

Equation 4 is a reasonable approximation only if a negligible pressure drop is found in the pumping chamber and through inlet and outlet valves and channels. But the most relevant assumption is that the pump is capable to pump all the stroke at any frequency. In fact, both electrostatic active expansion and passive elastic compression require a finite time. As a consequence, increasing the frequency over a limit value (which is a characteristic of the system) leads to a decrease of the effective amount of fluid which is pumped at each stroke. Experimental measurements on micropumps prototypes evidenced that the effects here neglected might assume a relevant role and then influence in a considerable manner micropump performances [9; 14].

If the maximum stroke v_s is taken as design parameter, a pumping efficiency index can be defined as

$$\mathcal{E}(f_p) = \frac{\Delta v(f_p)}{v_s} \cdot f_p \tag{6}$$

where $\Delta v \leq v_s$ represents the stroke obtained for a given pumping frequency. Finally, for a given design and pumping frequency f_p, the effective flow is

$$\mathcal{Q}(f_p) = v_s \cdot \mathcal{E}(f_p) \tag{7}$$

3 DEVICE MODELLING

In this work, dynamic electro-fluid-mechanical simulations are performed, with the aim to appreciate the effect of the fluid on device actuation. To the knowledge of the Authors, this is the first reported simulation of the fully coupled dynamic response of an electrostatic micropump.

An effective, sophisticated compact approach was proposed by Voigt *et al.* [15; 16]. To date, this is the only complete implemented model of the electrofluidic microsystem previously realized by Zengerle *et al.* [9]. Each component is a block, connected to the others in a Kirchoffian network, in which driving forces and resulting fluxes are treated with a lumped parameter approach. Each block is described by a physically based compact model extracted from continuum theory or from experimental data. Nevertheless, the lack of Finite Element simulations of the effective pumping mechanism does not enable a precise characterization of either the fluid dynamic field or the diaphragm action. Multiphysics Finite Element simulations can be used as a design tool not only to optimize the overall performance of the system, but also to reduce both the time and cost of development.

Due to the extreme aspect ratio of the device, a 3D multiphysics fully-coupled model has been found to be too expensive from the computational standpoint. In order to describe inlet and outlet while preserving flow directionality, an equivalent 2D plane strain model is defined which represents a diameter slice of the device. Parameters and constants adopted are reported in Table 1. Since the plane strain formulation exhibits a diaphragm flexural stiffness lower than the clamped circular plate, a scaling is necessary to obtain the same deflections as in the axisymmetric formulation. A straightforward solution is to scale Young's modulus, defining an equivalent modulus $E_{ps} = (8/3)\, E$ such that the maximum deflection obtained in plane strain simulations is the same that in the previously performed axisymmetric analysis [7]. With an out of plane equivalent chamber depth $d_f = \pi R/2$, the initial volume v_0 of the chamber is preserved. The volume $v(t)$ during actuation is in general larger, due to the different diaphragm deformed configuration, then it has to be scaled. The results can be considered a qualitative representation of the device dynamic behaviour. In fact, some relevant considerations can be drawn.

Second order quadrilateral elements are used for mechanical, electrostatic and fluid domains, with large displacements formulation and mesh movement described by the arbitrary Lagrangian-Eulerian scheme, with no remeshing. Characteristic length of the elements is $\ell \simeq h_m/10$. Suitable boundary conditions are defined along sub-domain boundaries, in terms of electrostatic forces and displacements (for the electro-mechanical interaction), and boundary velocities and fluid load (for the fluid-structure interaction).

E	polysilicon Young's modulus	160 GPa
ν	polysilicon Poisson's ratio	0.22
ρ	polysilicon density	2320 kg/m^3
ε	dielectric (air) permittivity	$8.854 \cdot 10^{-12}$ F/m
ρ_w	fluid (water) density	1000 kg/m^3
μ_w	fluid (water) viscosity	0.001 Pa $\cdot$ s

Table 1: Parameters and constants adopted in the Finite Element model.

4 RESULTS AND DISCUSSION

In Figure 4, square wave actuation is simulated at $f_p = 3$ Hz, for a device with $h_m = 30$ μm and $h_c = 6$ μm. Voltage is applied for half cycle, then switched off during the second half cycle. For this device geometry, this represents a limit frequency, beyond which the stroke volume can not be fully exploited. Indeed, if a higher actuation frequency is imposed, there is not enough time to reach equilibrium configuration at the end of neither expansion nor compression stroke. Increasing the frequency f_p, however, would improve the pumping performances: although a reduced stroke is exhibited, a higher number of pumping cycles is performed for a given time interval.

A set of simulations for different geometries, for actuation frequencies ranging from 1 Hz to 50 Hz with square wave actuation, is performed. This yield an estimate of the flow rate $\mathcal{Q}(f_p)$ in this simplified framework (Figure 5). As a first consideration, the micropump behaviour is well reproduced by the simplified 2D model here proposed, from a qualitative standpoint. In fact, it exhibits the same frequency trend found by the experimental results presented by Zengerle *et al.* [9] and Machauf *et al.* [14].

For low frequencies, here roughly below 1-5 Hz with respect to the device geometry, the full stroke is exploited. In this low-frequency regime, increasing the frequency of actuation corresponds to a proportional increase of flow rates. A further increase of the actuation frequency leads to a decrease of the stroke ($\Delta v \leq v_s$). This is initially overcompensated by faster actuation. When an optimal frequency is reached, the maximum of pumping effectiveness is achieved. A this point, a further increase of the actuation frequency f_p leads to a decrease of the generated fluid flow.

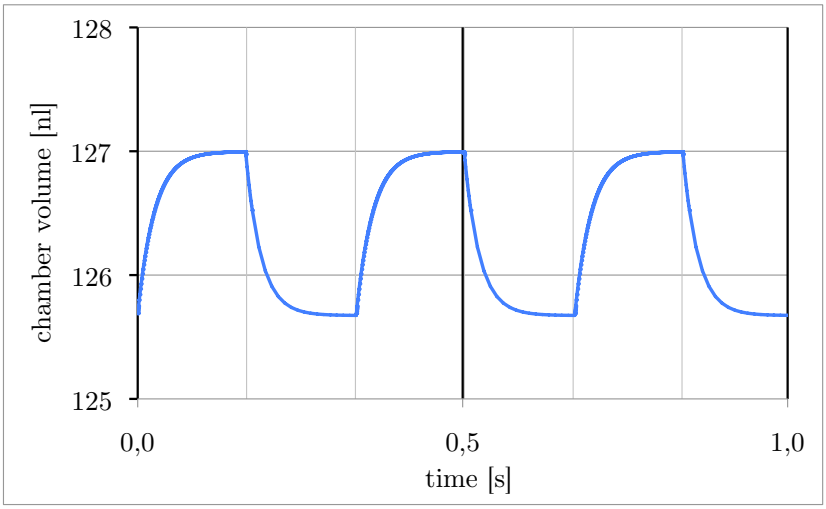

Figure 4: Chamber volume for square wave actuation at $f_p = 3$ Hz, for $h_m = 30$ μm and $h_c = 6$ μm.

From simulations, it appears that optimal pumping frequency is considerably influenced by membrane thickness, but not by capacitor spacing. For thinner diaphragms, a lower optimal actuation frequency is found. The obtained flow rate, for a given capacitor spacing, is the same in the investigated range of thickness. Although a higher stroke v_s is obtained with thinner diaphragms, this cannot be exploited at higher frequencies, due to pumped fluid inertia.

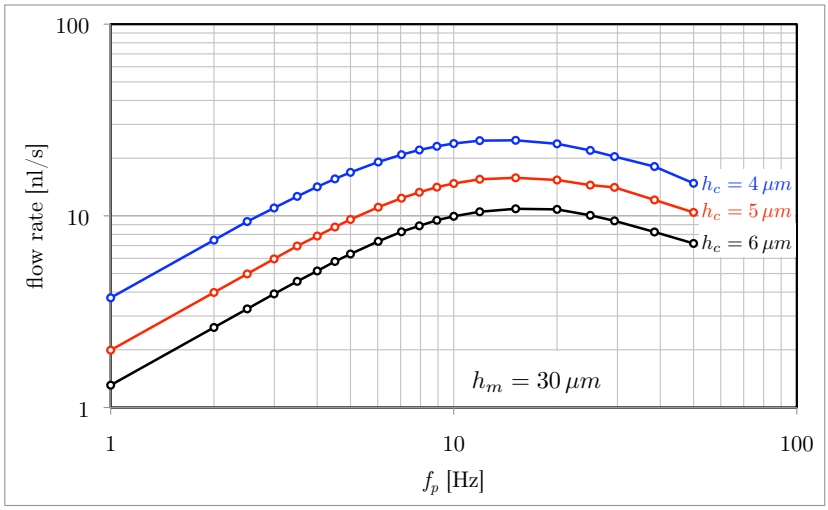

(a)

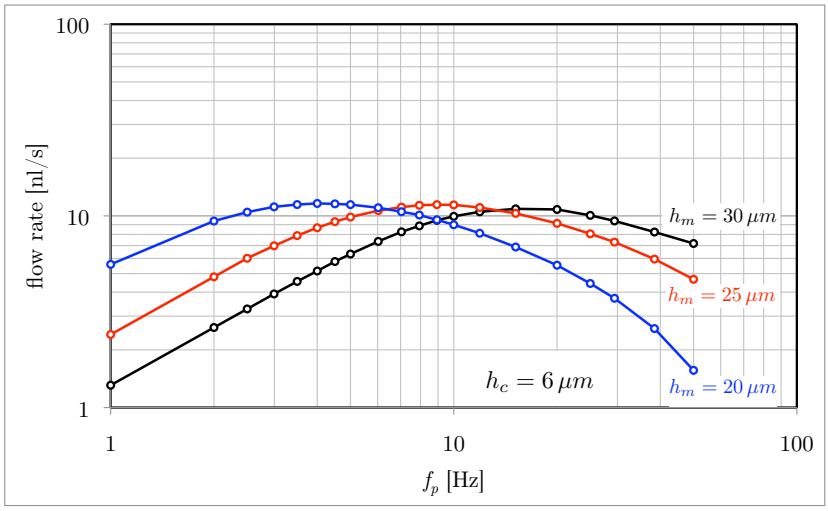

(b)

Figure 5: Flow rate $\mathcal{Q}(f_p)$ calculated by means of the dynamic fully-coupled electro-fluid-mechanical model. The effect of capacitor spacing h_c (a) and membrane thickness h_m (b) is emphasized.

On the other hand, the fluid transport capability is greatly influenced by the capacitor spacing, not by membrane thickness. As expected, for smaller gaps a higher actuation pressure is exerted and more liquid can be displaced. Moreover, dynamic simulations evidenced that the higher stroke v_s achieved by decreasing capacitor spacing is better exploited, since the optimal actuation frequency is the same in the investigated range of capacitor spacings (for a given membrane thickness).

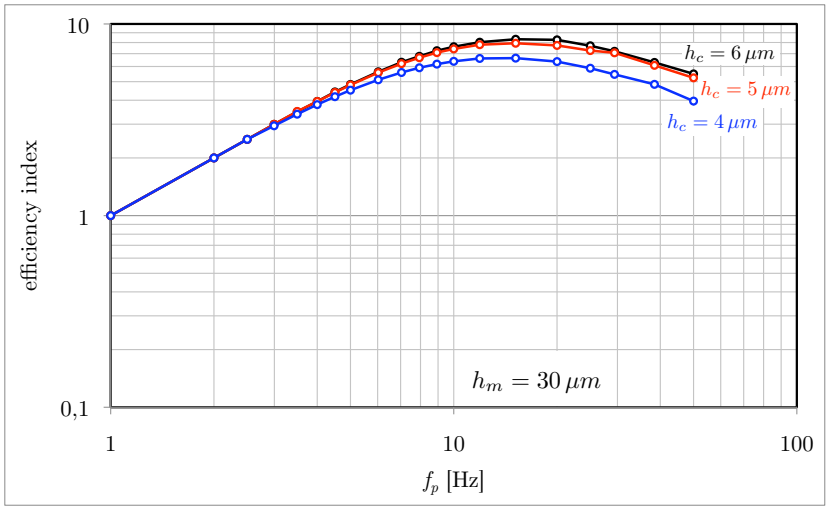

(a)

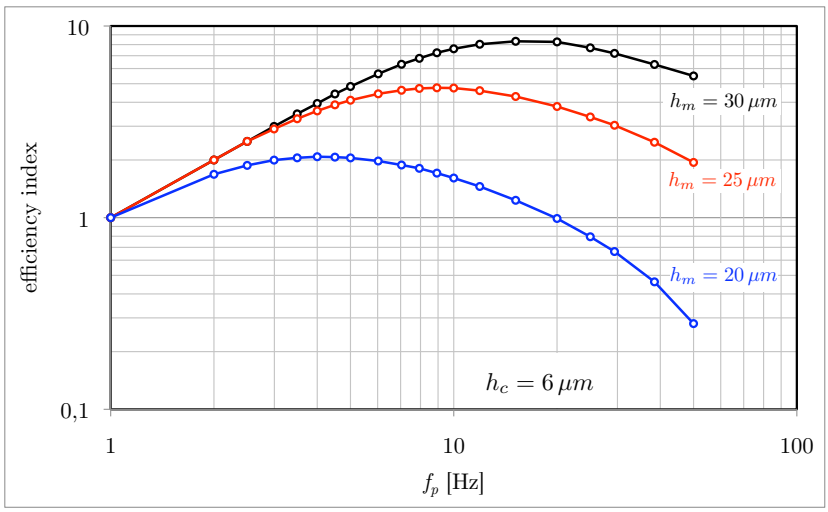

(b)

Figure 6: Efficiency index $\mathcal{E}(f_p)$ calculated by means of the dynamic fully-coupled electro-fluid-mechanical model. The effect of capacitor spacing h_c (a) and membrane thickness h_m (b) is emphasized.

Similar considerations can be drawn by considering the efficiency index $\mathcal{E}(f_p)$, plotted in Figure 6. The efficiency index, defined in Equation 6, is adopted here to quantify the advantage in improving the actuation frequency. It is clear that the micropump efficiency in the stable operation regime is greatly influenced by the membrane thickness h_m. Capacitor spacing has a reduced effect, that could became evident only for very small h_c. Considering dynamic effects and fluid inertia and referring to Equation 7, a flow rate $\mathcal{Q}$ of 1-2 μl/min can be hypothesized for the device, considerably lower that $\mathcal{Q}_i$ computed with standard arguments from quasi-static simulations.

5 CONCLUSIONS

In this work, a fully-silicon mechanical displacement micropump is investigated. From a technological standpoint, the final goal of the research project is to take advantage of well-established MEMS technologies and realize cost-effective and reliable devices which can directly integrate with both electronic and microfluidic components.

An investigation by means of numerical methods is performed to provide an outlook on the device fluid transport capabilities. This preliminary work is intended to support the design process and the prototype realization, by providing suggestions on the development of the device, in terms of working principle, geometric parameters, actuation voltage. As expected, the results suggest the possibility to adopt this device design for a proper fluid actuation, in terms of actuation voltages and geometry. For the considered geometry, a flow rate of 1-2 μl/min is expected for actuation frequencies from 10 to 30 Hz.

To take advantage of the full stroke, a maximum pumping frequency of 2-5 Hz can be hypothesized. A further increase of the actuation frequency leads to a decrease of the stroke ($\Delta v \leq v_s$), overcompensated by the faster actuation up to an optimal frequency, which corresponds to the maximum pumping effectiveness.

The optimal frequency identified for the current geometry is 10-30 Hz. A further increase of the actuation frequency f_p leads to a decrease of the generated fluid flow and a decay of performances. For a given actuation voltage in square wave, the optimal actuation frequency is greatly influenced by the membrane thickness h_m, but not by the capacitor spacing h_c. For thinner diaphragms, a lower optimal actuation frequency is found. By reducing the capacitor spacing h_c, higher flow rates can be obtained. The effect of membrane thickness h_m on the flow rate is negligible.

From a methodological point of view, it is worth to mention that the electro-fluid-mechanical dynamic simulations here presented return interesting results, although some rough simplifications are made to reduce the full problem to a 2D one. Indeed, to the knowledge of the Author, no detailed electro-fluid-mechanical fully-coupled models have been previously reported in the literature for electrostatic micropumps. The proposed simplified model is a step in this direction, and results are novel and encouraging.

To optimize the device and to improve pumping performances, the key component is the actuator, which deserves a particular attention. To increase the fluid transport capabilities dynamic drive could be exploited [17]. A viable alternative to increase the stroke volume avoiding pull-in is to apply charge control combined with tailored electrode shapes [18].

The device is here studied only in a stable range of actuation: a strong attention should be paid to pull-in phenomena, with the aim to control this feature and eventually to take advantage of it. The prototype developed by Zengerle and collaborators [9] works in the pull-in regime, developing a considerably higher stroke volume. In a similar circumstance, analyses should be performed to evaluate the adhesion (stiction) of the diaphragm and the its release after capacitor deactivation, also when the working fluid is present [19].

Acknowledgements

The Authors wish to acknowledge STMicroelectronics for the fruitful interaction in the development of this project.

References

[1] Iverson, B. and Garimella, S., Recent advances in microscale pumping technologies: a review and evaluation. *Microfluid. Nanofluid.* (2008) **5**:145–174.

[2] Woias, P., Micropumps – Past, progress and future prospects. *Sensor Actuat. B* (2005) **105**:28–38.

[3] Laser, D. and Santiago, J., A review of micropumps. *J. Micromech. Microeng.* (2004) **14**:R35–R64.

[4] Nisar, A., Afzulpurkar, N., Mahaisavariya, B. and Tuantranont, A., MEMS-based micropumps in drug delivery and biomedical applications. *Sensor Actuat. B* (2008) **130**:917–942.

[5] Zhang, C., Xing, D. and Li, Y., Micropumps, microvalves, and micromixers within PCR microfluidic chips: advances and trends. *Biotechnol. Adv.* (2007) **25**:483–514.

[6] Singhal, V., Garimella, S. and Raman, A., Microscale pumping technologies for microchannel cooling systems. *Appl. Mech. Rev.* (2004) **57**:191–221.

[7] Bertarelli, E., Ardito, R., Cioffi, M., Laganà, K., Procopio, F., Baldo, L., Corigliano, A., Contro, R. and Dubini, G., Design optimization of an electrostatic micropump: a multi-physics computational approach. In: *Proceedings of the 2nd South-East Conference on Computational Mechanics*, 181 & CD-ROM (2009).

[8] Oosterbroek, R., Schlautmann, S., Berenschot, J., Lammerink, T., van den Berg, A. and Elwenspoek, M., Modeling and validation of flow-structure interactions in

passive micro valves. In: *Technical Proceedings of the 1998 International Conference on Modeling and Simulation of Microsystems*, 528–533 (1998).

[9] Zengerle, R., Richter, A. and Sandmaier, H., A micro membrane pump with electrostatic actuation. In: *Proceedings of Micro Electro Mechanical Systems '92*, 19–24 (1992).

[10] Kotzar, G., Freas, M., Abel, P., Fleischman, A., Roy, S., Zorman, C., Moran, J. and Melzak, J., Evaluation of MEMS materials of construction for implantable medical devices. *Biomaterials* (2002) **23**:2737–2750.

[11] Bertarelli, E., Ardito, R., Bianchi, E., Laganà, K., Procopio, F., Baldo, L., Corigliano, A., Dubini, G. and Contro, R., A computational study for design optimization of an electrostatic micropump in stable and pull-in regime. *AES Tech. Rev. B: IJAMAIM* (2010) **1**:19–15.

[12] Cao, L., Mantell, S. and Polla, D., Design and simulation of an implantable medical drug delivery system using microelectromechanical systems technology. *Sensor Actuat. A* (2001) **94**:117–125.

[13] Teymoori, M. and Abbaspour-Sani, E., Design and simulation of a novel electrostatic peristaltic micromachined pump for drug delivery applications. *Sensor Actuat. A* (2005) **117**:222–229.

[14] Machauf, A., Nemirovsky, Y. and Dinnar, U., A membrane micropump electrostatically actuated across the working fluid. *J. Micromech. Microeng.* (2005) **15**:2309–2316.

[15] Voigt, P., Schrag, G. and Wachutka, G., Electrofluidic full-system modelling of a flap valve micropump based on Kirchhoffian network theory. *Sensor Actuat. A* (1998) **66**:9–14.

[16] Voigt, P., Schrag, G. and Wachutka, G., Microfluidic system modeling using VHDL-AMS and circuit simulation. *Microelectr. J.* (1998) **29**:791–797.

[17] Bertarelli, E., Ardito, R., Corigliano, A. and Contro, R., A plate model for the evaluation of pull-in instability occurrence in electrostatic micropump diaphragms. *Int. J. Appl. Mech.* (2011) **3**:1–19.

[18] Bertarelli, E., Corigliano, A., Greiner A. and Korvink, J.G., Design of high stroke electrostatic micropumps: a charge control approach with ring electrodes. *Microsyst. Technol.* (2011) **17**:165–173 .

[19] Ardito, R., Bertarelli, E., Contro, R. and Corigliano, A., Static and dynamic analyses of actuation devices in electrostatic micro-pumps. In: *Proceedings of the 7th International Conference on Engineering Computational Technology*, paper 121 (2010).